# Bioplastic Production Potential of *Azospira suillum* PS: Growth-Associated PHB Production Under Aerobic and Anaerobic Conditions

**David A.O. Meier[1], Benjamin Glazer[1], V. Celeste Lanclos[1], Hans K. Carlson[2], John D. Coates[1*]**

[1] Department of Plant and Microbial Biology, University of California, Berkeley, Berkeley, CA, United States

[2] Environmental Genomics and Systems Biology Division, Lawrence Berkeley National Laboratory, Berkeley, CA, United States

*** Correspondence:** John D. Coates (jdcoates@berkeley.edu), Department of Plant and Microbiology, 241 Koshland Hall, University of California, Berkeley, CA; Tel +1-510-643-8455

**Competing Interests Statement:**

The authors do not declare any competing interests.

## Abstract

Plastics are indispensable in modern society, yet less than 10% of the 380 million tons produced annually are recycled. This accumulation of non-degradable waste has intensified the search for sustainable alternatives. Polyhydroxyalkanoates (PHAs), particularly polyhydroxybutyrate (PHB), are biodegradable polymers produced by microorganisms. Here, we investigate the capacity of *Azospira suillum* PS, a model facultative perchlorate-reducing bacterium, to synthesize PHB. We show that unlike most organisms, PHB production is growth-associated both aerobically, and anaerobically with perchlorate as an electron acceptor under moderate nitrogen deplete conditions. Genomic analysis revealed four *phaC* homologs, with one, *phaC4,* co-localized with *phaB* and *phaR*, suggesting a conserved operon. While three of the *phaC* genes were successfully deleted, *phaC4* could not be disrupted, indicating an essential role for growth. Redox profiling revealed a positive correlation between PHB accumulation and $NADPH/NADP^+$ ratios, supporting the role of cytoplasmic reducing equivalents in PHB synthesis. This study presents the first demonstration of PHA production under perchlorate-respiring conditions and one of the few documented cases of growth-associated PHA synthesis. It offers new insights into the genetic and metabolic basis of PHB production in *A. suillum* PS, underscoring its potential as a platform organism for sustainable, growth-coupled bioplastic production.

## Introduction

The use of processed polymers by humans dates to at least 1600 B.C.E. (Hosler et al., 1999), but the invention of modern thermoplastics by Charles Goodyear in 1839 revolutionized their industrial and environmental impact. Today, thermoplastics are indispensable across nearly every sector due to their lightweight, durable, and versatile properties (Andrady & Neal, 2009). This utility has driven global plastic production to over 380 million tons annually (Geyer et al., 2017). However, nearly all conventional plastics are derived from fossil hydrocarbons and are non-biodegradable, leading to long-term environmental accumulation. This persistent pollution, along with the carbon footprint associated with petrochemical feedstocks, has accelerated interest in sustainable alternatives such as bioplastics—materials synthesized from renewable sources.

Polyhydroxyalkanoates (PHAs) are one such family of bioplastics that are fully compostable, produced by microorganisms as intracellular carbon and energy storage polymers (Macrae & Wilkinson, 1958). PHAs are classified by monomer length into short-chain-length (scl-PHA, C3–C5) and medium-chain-length (mcl-PHA, C6–C14) types, with copolymers offering diverse material properties (Steinbüchel, 1991; Chen et al., 2015; McAdam et al., 2020). This chemical versatility allows tailoring of rigidity, flexibility, and degradability for various applications (Gao et al., 2011). However, commercial PHA adoption is constrained by cost of production—typically $3–8 per kg in 2025, compared to ~$1.40 for petrochemical polyethylene—with global production representing less than 0.5% of total plastics (Rosenboom et al., 2022). Reducing cost of production through improvement of microbial titers and yields requires deeper insight into PHA biosynthetic regulation and physiology.

Among PHAs, polyhydroxybutyrate (PHB) is the best studied, first identified in *Bacillus subtilis* in 1926 (Lemoigne). Since then, PHAs have been detected in diverse bacteria (both autotrophs and heterotrophs), archaea (Poli et al., 2011), and some yeasts (Thu et al., 2023), where they typically accumulate under nutrient-limiting, carbon-rich conditions. PHB biosynthesis involves a core pathway encoded by *phaA* (β-ketothiolase), *phaB* (acetoacetyl-CoA reductase), and *phaC* (PHA synthase), which polymerizes 3-hydroxybutyryl-CoA. Additional regulators such as *phaR* and granule-associated *phaP* (phasin) influence polymer accumulation and granule morphology (Pötter et al., 2005). PHA synthases (PhaC enzymes) are grouped into four classes (I–IV) based on their substrate specificity and subunit composition, rather than their evolutionary lineage. Classes I, III, and IV primarily synthesize short-chain-length PHAs like PHB but differ in enzyme architecture: Class I enzymes are homodimers composed of two identical PhaC subunits; Class III enzymes function as heterodimers consisting of PhaC and a partner protein, PhaE; and Class IV enzymes also form heterodimers, pairing PhaC with PhaR. In contrast, Class II enzymes are specialized for producing medium-chain-length PHAs and typically include multiple PhaC isoforms (e.g., PhaC1 and PhaC2), without accessory subunits like PhaE or PhaR. A deeper understanding of how feedstock composition and PHA synthase structure influence polymer diversity and accumulation remains a key research goal.

*Cupriavidus necator* H16 is a model PHA producer and has been extensively engineered for high PHB yields (Zhang et al., 2022). Strategies include promoter and pathway optimization (Tang et al., 2020), substrate engineering (Mifune et al., 2010), and process development (Atlić et al., 2011). However, a key limitation is that PHB production in *C. necator* is not growth-associated, requiring nutrient shifts or batch processes, which hinders continuous cultivation (Henderson & Collins, 1997) and thus loss in industrial efficiency. Broader surveys have revealed PHA production in extremophiles, anaerobes, and oligotrophs (Wang et al., 2019a; Bennett et al., 2024), suggesting that novel chassis organisms with more favorable production dynamics remain to be explored.

Dissimilatory perchlorate-reducing bacteria (DPRB) represent a promising but understudied group in this context. Perchlorate ($ClO_4^-$) is a highly oxidized, water-soluble oxyanion with a biological redox potential comparable to oxygen ($E^{\circ\prime} = +0.797$ V) (Youngblut et al., 2016). In DPRB, perchlorate is reduced to chlorite by the perchlorate reductase complex (PcrAB), followed by dismutation into chloride and molecular oxygen via chlorite dismutase (Cld). The oxygen is subsequently respired by the microorganism (Youngblut et al., 2016). This pathway enables the endogenous generation of $O_2$ under anoxic conditions, supporting oxygenase-dependent metabolism without external aeration (Carlström et al., 2015). The conserved, mobile perchlorate reduction island (PRI) allows this metabolism to be transferred across diverse taxa, supporting bioengineering efforts (Melnyk et al., 2015). *Azospira suillum* PS is a facultative anaerobe and genetically tractable DPRB

83 capable of coupling perchlorate reduction to energy conservation and growth. Despite its unique
84 metabolism and flexible redox physiology, its potential for bioproduct synthesis remains unexplored.

85 In this study, we investigate the genetic and physiological basis of PHB biosynthesis in *A.*
86 *suillum* PS. Using comparative genomics, gene deletion, redox analysis, and polymer quantification,
87 we characterize the pathways supporting PHB production during both aerobic and perchlorate-
88 respiring growth. Our findings highlight *A. suillum* PS as a unique candidate for sustainable, growth-
89 coupled bioplastic production in anaerobic biotechnological systems.

## 90 Materials and Methods

### 91 Bacterial Strains and Plasmids

92 *Azospira suillum* PS (ATCC BAA-33/DSMZ 13638) was revived from laboratory freezer
93 stocks and used as the wild-type strain for all genetic manipulations. *Escherichia coli* XL1-Blue was
94 used for plasmid propagation and cloning. A full list of primers (Supplementary Table 1), strains
95 (Supplementary Table 2), and plasmids (Supplementary Table 3) is provided in the supplementary
96 materials. Prior to all experiments, strains were streaked from freezer stocks to obtain single colonies.

### 97 Mutant Construction

98 Gene deletion mutants in *A. suillum* PS were generated using a sacB-based counterselection
99 approach (Gay et al., 1983). Electrocompetent cells were transformed with either integrative (~500
100 ng) or replicative (~50 ng) plasmids in 1 mm electroporation cuvettes using a Gene Pulser Xcell
101 electroporator (Bio-Rad, USA) with the following settings: 1.8 kV, 25 µF, and 200 Ω. Cells were
102 chilled on ice before electroporation; cuvettes were kept at room temperature. After pulsing, cells
103 were recovered in pre-warmed ALP medium at 37°C for 6 h, then 100 µL of culture was plated
104 directly on ALP agar containing 50 µg/mL kanamycin. Colonies appearing within 48 h were
105 considered valid transformants and picked into 500 µL ALP broth with 50 µg/mL kanamycin. After 4
106 h of growth, cultures were plated on ALP agar with 6% sucrose for counterselection. Representative
107 colonies were screened by colony PCR to confirm deletions. Glycerol stocks were prepared at 15%
108 final concentration for storage at −80°C.

### 109 Culture Conditions and Growth Media

110 *E. coli* strains were cultured in LB medium with 50 µg/mL kanamycin. Wild-type and mutant
111 *A. suillum* PS strains were grown in acetate minimal medium (AMM). One liter of AMM contained:
112 0.49 g sodium phosphate monobasic dihydrate, 0.97 g sodium phosphate dibasic anhydrous, 0.1 g
113 KCl, 0.25 g $NH_4Cl$, and 10 mL each of vitamin and mineral mix (Bruce et al., 1999). The sodium
114 acetate concentration in AMM was either 0.82g/L acetate for 10mM AMM or 2.05 g acetate for
115 25mM AMM. To prepare mixed carbon source media (acetate, lactate, pyruvate), AMM was
116 supplemented with 2.0 g yeast extract, 7.6 mL of a 60% (w/w) sodium lactate solution, and 1.10 g
117 sodium pyruvate. For solid media, 15 g/L agar was added. *A. suillum* PS was cultured in 250 mL
118 baffled Erlenmeyer flasks containing 50 mL of medium at 37°C and 250 rpm. Optical density at 600
119 nm ($OD_{600}$) was measured using a 1 mm pathlength cuvette on a Genesys 20 spectrophotometer
120 (Thermo Scientific, USA).

121 **PHA Extraction and GC-MS Analysis**

122 PHB was quantified from 40 mL of culture. Samples were harvested by centrifugation at 7,197
123 × g for 10 min at 4°C, and pellets were stored at −80°C. Acidic methanolysis was performed as
124 described by Juengert et al. (2018). Extracts were analyzed by GC-MS using a 7890A GC system
125 (Agilent Technologies, USA) equipped with a DB-WAX UI column and coupled to a 5975C XL
126 EI/CI Mass Selective Detector. The temperature program was: 80°C for 2 min, ramp to 210°C at
127 10°C/min, then to 250°C at 50°C/min with a 1 min hold. Poly[(R)-3-hydroxybutyric acid] (Santa
128 Cruz Biotechnology, USA) was used for the standard curve, and methyl benzoate (Sigma-Aldrich,
129 USA) served as the internal standard. Compound identity was confirmed by total ion count (TIC)
130 spectra matching the NIST EI database. The presence of polyhydroxyvalerate (PHV) and
131 polyhydroxyhexanoate PHHX was assessed using a commercial PHA standard (Sigma-Aldrich,
132 USA), and TIC peaks were compared with NIST spectra for 3-hydroxypentanoic acid methyl ester
133 and 3-hydroxyhexanoic acid methyl ester.

134 **$NAD(P)^+$/H Quantification**

135 Redox metabolite analysis was performed as described by Kern et al. (2014). Samples were
136 kept on ice and protected from light until incubated at 37°C. To prevent redox degradation, only three
137 samples were processed at a time. Quantification was performed using a Varian Cary 50 MPR
138 Microplate Reader (Agilent Technologies, USA).

139 **Fluorescence Microscopy**

140 Microscopy was conducted as described by Juengert et al. (2018). Cells were harvested in
141 exponential phase, washed once in PBS (8 g NaCl, 201 mg KCl, 1.42 g $Na_2HPO_4$, 245 mg $KH_2PO_4$
142 per liter, pH 7.4), and stained with 1 µg/mL Nile Red for 10 min in the dark. Samples were mounted
143 on 1% agarose pads and visualized on a Zeiss LSM880 confocal microscope (Zeiss, Germany) using
144 a 100× Plan-Apochromat NA 1.4 objective. Nile Red was excited at 561 nm, and emission was
145 detected from 570–620 nm using a GaAsP photon-counting detector. Differential interference
146 contrast (DIC) images were acquired simultaneously. Image acquisition settings were consistent
147 across all samples and processed in ZEN software v2.3 SP1 (Zeiss).

148 **Phylogenetic Tree Construction**

149 Each *phaC* gene from *A. suillum* PS was queried against the NCBI nr database using BLASTP
150 (Altschul et al., 1990). The top 250 unique hits (excluding "multispecies" entries) were retained per
151 gene. PhaC homologs from *Azospira* species were manually reviewed and validated using HMMER
152 v3.4 with TIGRfam-specific models (Finn et al., 2011). Alignments were generated with MUSCLE
153 v3.8.31 and trimmed using trimAl v1.4 (Edgar, 2004; Capella-Gutiérrez et al., 2009). Phylogenies
154 were inferred using IQ-TREE v2.0.6 with 1,000 ultrafast bootstraps and the Q.pfam+I+R7 model.
155 Trees were visualized using iTOL v6 (Minh et al., 2020; Letunic and Bork, 2020).

156 **In Silico Comparative Genomics**

157 The genome of *A. suillum* PS was downloaded from NCBI (Sayers et al., 2024);
158 *Dechloromonas agitata* CKB and additional *Azospira* genomes were retrieved from JGI-IMG
159 (Markowitz et al., 2006). Genomes were searched using HMMER v3.4 with a custom set of

160 TIGRfams relevant to PHA metabolism (Supplementary Table 4). Presence/absence patterns of PHA
161 biosynthesis genes were visualized using R v4.4.2 and RStudio v2024.12.0+467.

162 **Results**

163 **Genomic and microscopic evidence for PHB granule formation in *Azospira suillum* PS and other**
164 **perchlorate-reducing bacteria**

165 Previous work on the perchlorate-reducing bacterium *Dechloromonas agitata* CKB revealed
166 electron-dense intracellular structures that were hypothesized to be PHA granules (Fig. 1a) (Bruce et
167 al., 1999). *In silico* analysis (Fig. 1) confirmed that *D. agitata* CKB possesses all the core genes
168 necessary for PHA biosynthesis, including *phaA*, *phaB*, *phaC*, *phaP*, and *phaR*, which together enable
169 the conversion of acetyl-CoA to PHB and the regulation and granule-associated assembly of PHA. To
170 further investigate this capacity in a more genetically tractable system, we turned to *Azospira suillum*
171 PS, a model perchlorate-reducing bacterium with established genetic tools (Melnyk et al., 2014). Strain
172 PS also contains the requisite genes for PHA biosynthesis (Fig. 1); however, unlike CKB, it
173 additionally encodes the PHA depolymerase *phaZ*. Both organisms possess multiple copies of the *phaC*
174 gene—three in CKB and four in PS (see Supplementary Table 5 for locus tags in PS). In both strains,
175 one *phaC* copy is co-localized with *phaB* and *phaR* (Fig. 1), suggesting an operon structure, while the
176 remaining *phaC* copies are dispersed throughout the genome. Of these, only one has a neighboring
177 *phaP* gene, and no other adjacent genes associated with PHA biosynthesis were observed.

178 To determine whether *A. suillum* PS produced PHB granules, we stained cultured cells with
179 Nile Red, a lipophilic dye commonly used to visualize PHB granules and examined them using
180 confocal microscopy (Fig. 1b). PS cells exhibited visible intracellular PHB granules with an
181 approximate diameter of 0.32 µm. Given the ~2 µm cell diameter of PS, the clustered granules span
182 much of the intracellular space, corresponding to ~64% of the estimated cell volume being occupied
183 by PHB granules. Cells stained positive for PHB granules under both aerobic and perchlorate-respiring
184 conditions, providing the first clear evidence of PHA production linked to perchlorate respiration. This
185 observation confirmed the genetic potential for PHB accumulation; however, it remained unclear
186 whether polymer synthesis occurred constitutively or only in response to specific nutrient conditions.

187 To establish whether PHB accumulation in *A. suillum* PS is constitutive or nutrient-dependent,
188 we first evaluated growth under nitrogen-replete conditions. Cultures were grown in standard acetate
189 minimal medium (AMM) containing 10 mM sodium acetate and 4.68 mM $NH_4Cl$, corresponding to a
190 replete C:N ratio of approximately 1:0.23 relative to the canonical Redfield ratio (C:N = 1:0.15)
191 (Redfield, 1934). Under these conditions, no detectable PHB was observed by GC–MS analysis (Fig.
192 1d), confirming that PHB synthesis does not occur under nitrogen-replete growth. The culture exhibited
193 a specific growth rate (µ) of 0.60 $h^{-1}$ and a doubling time of 1.16 h, indicating robust biomass formation
194 despite the absence of polymer accumulation.

195 Given prior genomic and microscopic evidence suggesting PHB-producing potential, we next
196 examined whether altering the carbon-to-nitrogen ratio could induce polymer synthesis. When the
197 acetate concentration was increased to 25 mM while maintaining 4.68 mM $NH_4Cl$ (C:N= 1:0.094),
198 PHB production was observed under both aerobic and perchlorate-respiring conditions (Fig. 2a–d).
199 Under these carbon-enriched conditions, cell experience ~38% less nitrogen per unit carbon than
200 under the canonical Redfield ratio, experiencing moderate nitrogen limitation. Under these conditions
201 *A. suillum* PS exhibited a slightly reduced specific growth rate (µ = 0.50 $h^{-1}$; doubling time = 1.39 h)
202 but accumulated measurable intracellular PHB. These results demonstrate that PHB synthesis in *A.*

203 *suillum* PS is triggered by a shift toward carbon surplus relative to nitrogen, rather than being a
204 constitutive feature of its metabolism.

205 Following this finding, we conducted a detailed time-course analysis of PHB accumulation
206 under the carbon-enriched condition to quantify the extent and dynamics of polymer synthesis during
207 aerobic and perchlorate-respiring growth.

208 **Growth-associated PHB production in *Azospira suillum* PS under aerobic and perchlorate-**
209 **respiring conditions**

210 To quantify PHA production by *A. suillum* PS, gas chromatography–mass spectrometry (GC-
211 MS) was performed on samples extracted via acidic methanolysis. In addition to quantifying total PHB
212 produced by the culture, this method also enabled identification of the different monomers present.
213 When PS was grown on acetate under either aerobic or perchlorate-respiring conditions 3-
214 hydroxybutyric acid (3-HB) (the monomer of PHB) was detected. PHB was quantified across the
215 growth curve and was found to be produced in a growth-associated manner (Fig 2a-d). While growth-
216 associated PHB production has been previously reported (Scott et al., 2021; Amos & McInerney, 1989;
217 Ackermann & Babel, 1997); PHB biosynthesis is more commonly observed during stationary phase,
218 in response to nutrient limitation (Anderson & Dawes, 1990).

219 When grown aerobically, *A. suillum* PS reaches a maximum $OD_{600nm}$ of 0.747 ± 0.008 during
220 late exponential phase, at which point it had produced a maximum of 0.077 ± 0.006 mg/mL PHB
221 providing a total yield of 0.10 g/L per $OD_{600nm}$ (Fig 2a). Under perchlorate-respiring conditions with
222 10 mM perchlorate, PS reaches a lower maximum $OD_{600nm}$ of 0.397 ± 0.009 and produces a
223 maximum of 0.024 ± 0.008 mg/mL PHB or 0.06 g/L per $OD_{600nm}$ (Fig 2b). When grown on
224 perchlorate, PHB levels slightly decline as the culture enters stationary phase (Fig 2d). There is no
225 significant reduction in PHB levels between peak and late-stage culture under aerobic conditions,
226 despite a drop in $OD_{600nm}$ of approximately 0.21. Based on the 1.6-fold higher PHB yield in aerobic
227 versus perchlorate conditions, we further characterized PHB production by PS under aerobic growth.

228 This growth-associated pattern under carbon-enriched conditions contrasts with the nitrogen-
229 replete culture, where no PHB was detected, reinforcing that polymer synthesis in *A. suillum* PS is
230 activated only when the C:N ratio exceeds a physiological threshold. Under both mild and severe
231 nitrogen limitation, PHB production remained unchanged, which is consistent with observations in
232 other anaerobic organisms such as *Syntrophomonas wolfei*, which produced PHB independently of
233 ammonium chloride concentration (Amos & McInerney, 1989).

234 When examining normalized PHB levels relative to optical density, both aerobic and
235 perchlorate-grown cultures show evidence of carryover PHB from the inoculum (Fig 2c&d). In
236 aerobic cultures, this residual PHB is rapidly degraded during lag phase prior to new PHB
237 accumulation during log phase, suggesting that the cells may utilize the carryover PHB as an
238 additional electron donor alongside the supplied acetate during the initial phase of growth (Fig 2c). In
239 contrast, perchlorate-respiring cultures do not exhibit this initial degradation phase; instead,
240 normalized PHB/$OD_{600}$ remains stable during early growth and begins increasing only during
241 exponential phase.

242 **Redox cofactor dynamics link NADPH availability to PHB biosynthesis in *Azospira suillum* PS**

To assess the redox influence on PHB biosynthesis, we measured intracellular $NADH/NAD^+$ and $NADPH/NADP^+$ ratios over a 24-hour culture period and compared these values to PHB accumulation (Fig. 3a–d). When grown aerobically, *Azospira suillum* PS exhibited an average $NADH/NAD^+$ ratio of 0.491—more than twice the reported aerobic values for *E. coli* (0.226) and *Klebsiella aerogenes* (0.195)—indicating a relatively reduced intracellular environment. Notably, this ratio also exceeded those observed under anaerobic conditions for both comparative organisms (0.396 and 0.219, respectively) (Wimpenny & Firth, 1972). Only *Pseudomonas aeruginosa*, a known respiratory generalist, exhibited a higher aerobic $NADH/NAD^+$ ratio (0.571). While *E. coli* lacks the genetic capacity for native PHA production, some *Pseudomonas* spp. are known PHB producers, although not typically in a growth-associated fashion (Bertrand et al., 1990).

Spearman correlation analysis revealed a strong and statistically significant monotonic relationship between PHB levels and $NADPH/NADP^+$ ($\rho = 0.829$, $p = 0.042$), while no significant correlation was observed with $NADH/NAD^+$ ($\rho = 0.600$, $p = 0.208$). This is consistent with the known cofactor specificity of the PhaB acetoacetyl-CoA reductase enzyme. In *Cupriavidus necator* H16—a well-studied model organism for PHB production—this enzyme has been shown to preferentially use NADPH rather than NADH as the reducing equivalent source (Steinbüchel & Schlegel, 1991).

**Phylogenomic analysis reveals conserved, diversified *phaC* loci across the *Azospira* genus**

A maximum-likelihood phylogenetic tree (Fig 4) constructed from the four unique *phaC* gene products identified in *Azospira suillum* PS, along with their 250 closest homologs, revealed that each PhaC protein is nested within a monophyletic clade composed of *phaC* homologs from other *Azospira* species. Despite this shared genus-level affiliation, the four *phaC* variants from strain PS occupy distinct and divergent branches within the tree, suggesting that each *phaC* gene may have evolved independently. Furthermore, this analysis revealed that multiple *phaC* gene copies are consistently present in *Azospira* genomes. Comparative genomic analysis across the genus showed that each *Azospira* species encodes at least three distinct copies of *phaC*, alongside a single copy of the transcriptional regulator *phaR*, suggesting that PHA biosynthesis is a conserved metabolic feature within the genus. To assess whether these genes may have been acquired via horizontal gene transfer, we used IslandViewer (Bertelli et al., 2017), which predicts genomic islands based on sequence composition and comparative genomics. This analysis showed no evidence of horizontal gene transfer near the *phaC* loci in strain PS (data not shown).

To assess conservation of gene neighborhoods, we used CAGE-CAT and Clinker to compare the genomic loci surrounding *phaC* across *Azospira* genomes (Gilchrist & Chooi, 2021). These tools align and visualize syntenic regions based on protein sequence identity and gene order, enabling rapid identification of conserved operons and structural rearrangements. This analysis (Fig 5) revealed that the local gene context of *phaC* is highly conserved, with pairwise amino acid identity of *phaC* homologs exceeding 70% across the genus, further supporting their functional importance in *Azospira*. However, while average nucleotide identity remains high across *Azospira* species, they do not share syntenic conservation of the broader PHA biosynthesis gene cluster.

**Functional characterization of *phaC* genes reveals essential role of *phaC4* in PHB biosynthesis**

Our analysis found that *Azospira suillum* PS encodes only class I *phaC* genes, which are typically associated with the production of short-chain-length (scl) PHAs such as PHB. To investigate the four *phaC* genes in *A. suillum* PS responsible for PHA production, we attempted to

286 generate deletion mutants for each gene. Knockout strains were successfully constructed for three out
287 of the four *phaC* genes. However, under all tested growth conditions, we were unable to generate a
288 mutant lacking the *phaC* gene with the locus tag *dsui_2537* (*phaC*4). Notably, this gene is co-
289 localized with *phaB* and *phaR*. Previous transposon mutagenesis studies in strain PS also identified
290 *phaC*4 as essential under all conditions tested (Supplementary Figure 1).

291 To further assess the functional role of each *phaC*, we compared the PHA monomer profiles
292 of all knockout strains under both defined and complex media conditions. As shown in Table 1, none
293 of the knockout strains displayed a PHA profile distinct from wild type. All strains consistently
294 produced PHB, while polyhydroxyvalerate (PHV) and polyhydroxyhexanoate (PHHX) were absent
295 (data not shown). These results suggest that the essential *phaC*4 is playing an important physiological
296 role during normal growth in nutrient replete media.

297 **Discussion**

298 This study provides new insight into the biosynthesis and regulation of polyhydroxybutyrate
299 (PHB) in *Azospira suillum* PS, a model perchlorate-reducing bacterium. We demonstrate for the first
300 time that PHB biosynthesis occurs under perchlorate-respiring conditions, expanding the known
301 metabolic range for polyhydroxyalkanoate (PHA) production. Notably, *A. suillum* PS accumulates
302 PHB in a growth-associated manner under both aerobic and anaerobic conditions, with aerobic
303 cultures producing 1.6-fold more PHB. PHB synthesis was absent under nitrogen-replete conditions
304 and was only observed when the carbon-to-nitrogen ratio was altered to a ~40 % reduction in
305 nitrogen availability relative to the canonical Redfield ratio. This establishes that PHB production in
306 *A. suillum* PS is triggered by moderate nutrient imbalance. This pattern contrasts with the stress-
307 induced, stationary-phase accumulation commonly observed in other bacteria, such as *C. necator*,
308 suggesting that PHB plays a role in the central metabolism of *A. suillum* PS under nitrogen limitation
309 where it is coupled to growth under both aerobic and perchlorate reducing conditions.

310 Temporal analysis of PHB accumulation revealed distinct regulatory patterns between
311 respiratory modes. Under aerobic growth, normalized PHB/$OD_{600}$ initially declines during lag phase,
312 likely reflecting mobilization of stored carbon and reducing equivalents. In contrast, perchlorate-
313 respiring cultures do not exhibit this early decrease; instead, PHB levels remain stable in early
314 growth and begin to rise during exponential phase.

315 Our redox profiling data support this hypothesis. A strong and statistically significant
316 correlation was observed between intracellular $NADPH/NADP^+$ ratios and PHB content (Spearman $\rho$
317 $= 0.829$, $p = 0.042$), implicating NADPH availability as a potential driver of PHB accumulation.
318 Although this observation suggests a role for NADPH in fueling PHB biosynthesis, this correlation
319 does not confirm cofactor specificity of the biosynthetic enzymes. NADH and NADPH levels are
320 often tightly coupled and metabolically interconvertible, and the observed association may reflect a
321 broader redox state rather than direct NADPH usage. Further biochemical characterization will be
322 required to determine whether PhaB or related enzymes in *A. suillum* PS preferentially utilize
323 NADPH over NADH.

324 Genomic analysis revealed four *phaC* genes encoding class I PHA synthases in *A. suillum* PS.
325 Of these, *phaC4* is particularly notable for its synteny with *phaB* and *phaR*, suggesting a conserved
326 operon structure. No evidence of horizontal gene transfer was detected near any *phaC* loci, indicating
327 that these genes are native and vertically inherited. Functional analysis supports the essentiality of
328 *phaC4*, as multiple attempts to generate a knockout mutant were unsuccessful under all tested

329 conditions. These findings further reinforce the hypothesis that PHB biosynthesis plays a central
330 physiological role in this organism, potentially as a buffer for intracellular reducing equivalents.

331 From an applied perspective, *A. suillum* PS demonstrates rapid and efficient PHB accumulation
332 on simple substrates. Under aerobic conditions, wild-type PS produces 8.5 mg/L/h PHB, reaching
333 77 mg/L in just 9 hours using a single 25 mM acetate dose (600 mg/L carbon). While this yield is
334 lower than that of *Cupriavidus necator*—which reaches up to 79.2 mg/L/h on soybean oil after 72
335 hours—*C. necator* requires multiple feedings totaling ~7,000 mg/L carbon (Mifune et al., 2010),
336 greater than tenfold more than the PS culture. In contrast, PS grows in minimal medium without
337 supplementation, avoiding the cost and handling challenges of plant oils. These characteristics
338 position *A. suillum* PS as a promising chassis for continuous, low-input bioplastic production.

339 With targeted metabolic engineering—such as overexpression of *phaCBR* and optimization of
340 carbon feed strategies—*A. suillum* PS may achieve higher titers while retaining its growth-associated
341 PHB phenotype. This production strategy is particularly well-suited for bioprocesses favoring
342 continuous synthesis and redox-balanced metabolism. Overall, our findings position *A. suillum* PS as
343 a novel and sustainable chassis for industrial PHA production, especially in systems where
344 simplicity, growth-coupling, and cost-effective carbon utilization are critical design goals.

345 **Industrial relevance**

346 This study identifies *Azospira suillum* PS as a promising new chassis for sustainable
347 bioplastic production. Unlike most known PHA producers, *A. suillum* PS accumulates PHB in a
348 growth-associated manner under both aerobic and anaerobic (perchlorate-respiring) conditions,
349 enabling simpler, continuous fermentation processes. Its ability to produce PHB rapidly on low-cost
350 substrates in minimal media, combined with native genetic tractability and redox-linked regulation,
351 makes it an attractive platform for scalable, low-input, and flexible biomanufacturing—particularly in
352 resource-limited or oxygen-poor environments.

353 **Conflict of Interest**

354 The authors declare no competing commercial, or financial interests in relation to the work presented
355 here.

356 **Author Contributions**

357 DAOM, HKC and JDC designed research. DAOM and BG optimized the genetic protocol and BG
358 constructed the mutants. DAOM and VCL generated the phylogenetic analysis. DAOM performed all
359 physiology experiments and measurements and comparative genomic analysis. DAOM wrote the
360 draft manuscript and created the figures with guidance from JDC. All authors contributed to data
361 analysis, reviewed the manuscript and approved of its publication.

362 **Funding**

363 Funding for this research was supported in part by generous sponsorship from the American Pacific
364 Corporation and the Baydin (Boomerang) Corporation.

365 **Acknowledgments**

The authors acknowledge Yi Liu for guidance on instrumentation and analyses, Dr. Denise Schichnes at the UC Berkeley Biological Imaging Facility for training and access to microscopy, and Dr. Ruiwen Hu for his advice on computational analyses.

## References

Achenbach, L A, U Michaelidou, R A Bruce, J Fryman, and J D Coates. "Dechloromonas Agitata Gen. Nov., Sp. Nov. and Dechlorosoma Suillum Gen. Nov., Sp. Nov., Two Novel Environmentally Dominant (per)Chlorate-Reducing Bacteria and Their Phylogenetic Position." *International Journal of Systematic and Evolutionary Microbiology* 51, no. 2 (March 1, 2001): 527–33. https://doi.org/10.1099/00207713-51-2-527.

Ackermann, J.-U., and W. Babel. "Growth-Associated Synthesis of Poly(Hydroxybutyric Acid) in Methylobacterium Rhodesianum as an Expression of an Internal Bottleneck." *Applied Microbiology and Biotechnology* 47, no. 2 (1997): 144–49. https://doi.org/10.1007/s002530050903.

Altschul, Stephen F., Warren Gish, Webb Miller, Eugene W. Myers, and David J. Lipman. "Basic Local Alignment Search Tool." *Journal of Molecular Biology* 215, no. 3 (October 5, 1990): 403–10. https://doi.org/10.1016/S0022-2836(05)80360-2.

Amos, Dale A., and Michael J. McInerney. "Poly-$\beta$-Hydroxyalkanoate in Syntrophomonas Wolfei." *Archives of Microbiology* 152, no. 2 (July 1989): 172–77. https://doi.org/10.1007/BF00456097.

Anderson, A. J., and E. A. Dawes. "Occurrence, Metabolism, Metabolic Role, and Industrial Uses of Bacterial Polyhydroxyalkanoates." *Microbiological Reviews* 54, no. 4 (December 1990): 450–72. https://doi.org/10.1128/mr.54.4.450-472.1990.

Atlić, Aid, Martin Koller, Dietrich Scherzer, Christoph Kutschera, Elizabeth Grillo-Fernandes, Predrag Horvat, Emo Chiellini, and Gerhart Braunegg. "Continuous Production of Poly([R]-3-Hydroxybutyrate) by Cupriavidus Necator in a Multistage Bioreactor Cascade." *Applied Microbiology and Biotechnology* 91, no. 2 (July 2011): 295–304. https://doi.org/10.1007/s00253-011-3260-0.

Bennett, Brittany D., David A.O. Meier, V. Celeste Lanclos, Hasti Asrari, John D. Coates, and J. Cameron Thrash. "Polyhydroxybutyrate Production in Freshwater SAR11 (LD12)." Microbiology, November 8, 2024. https://doi.org/10.1101/2024.11.08.622676.

Bertelli, Claire, Matthew R Laird, Kelly P Williams, Simon Fraser University Research Computing Group, Britney Y Lau, Gemma Hoad, Geoffrey L Winsor, and Fiona SL Brinkman. "IslandViewer 4: Expanded Prediction of Genomic Islands for Larger-Scale Datasets." *Nucleic Acids Research* 45, no. W1 (July 3, 2017): W30–35. https://doi.org/10.1093/nar/gkx343.

Bertrand, J.-L., B. A. Ramsay, J. A. Ramsay, and C. Chavarie. "Biosynthesis of Poly-β-Hydroxyalkanoates from Pentoses by *Pseudomonas Pseudoflava*." *Applied and Environmental Microbiology* 56, no. 10 (October 1990): 3133–38. https://doi.org/10.1128/aem.56.10.3133-3138.1990.

Bruce, Royce A., Laurie A. Achenbach, and John D. Coates. "Reduction of (per)Chlorate by a Novel Organism Isolated from Paper Mill Waste." *Environmental Microbiology* 1, no. 4 (August 1999): 319–29. https://doi.org/10.1046/j.1462-2920.1999.00042.x.

Byrne-Bailey, Kathryne G., and John D. Coates. "Complete Genome Sequence of the Anaerobic Perchlorate-Reducing Bacterium Azospira Suillum Strain PS." *Journal of Bacteriology* 194, no. 10 (April 25, 2012): 2767–68. https://doi.org/10.1128/jb.00124-12.

Capella-Gutiérrez, Salvador, José M. Silla-Martínez, and Toni Gabaldón. "trimAl: A Tool for Automated Alignment Trimming in Large-Scale Phylogenetic Analyses." *Bioinformatics (Oxford, England)* 25, no. 15 (August 1, 2009): 1972–73. https://doi.org/10.1093/bioinformatics/btp348.

Carlström, Charlotte I., Dana Loutey, Stefan Bauer, Iain C. Clark, Robert A. Rohde, Anthony T. Iavarone, Lauren Lucas, and John D. Coates. "(Per)Chlorate-Reducing Bacteria Can Utilize Aerobic and Anaerobic Pathways of Aromatic Degradation with (Per)Chlorate as an Electron Acceptor." Edited by Victor De Lorenzo and Sang Yup Lee. *mBio* 6, no. 2 (May 2015): e02287-14. https://doi.org/10.1128/mBio.02287-14.

Chen, Guo-Qiang, Juanyu Zhang, and Ying Wang. "White Biotechnology for Biopolymers." In *Industrial Biorefineries & White Biotechnology*, 555–74. Elsevier, 2015. https://doi.org/10.1016/B978-0-444-63453-5.00018-5.

Coates, John D., and Laurie A. Achenbach. "Microbial Perchlorate Reduction: Rocket-Fuelled Metabolism." *Nature Reviews Microbiology* 2, no. 7 (July 2004): 569–80. https://doi.org/10.1038/nrmicro926.

Edgar, Robert C. "MUSCLE: Multiple Sequence Alignment with High Accuracy and High Throughput." *Nucleic Acids Research* 32, no. 5 (2004): 1792–97. https://doi.org/10.1093/nar/gkh340.

Finn, Robert D., Jody Clements, and Sean R. Eddy. "HMMER Web Server: Interactive Sequence Similarity Searching." *Nucleic Acids Research* 39, no. suppl_2 (July 1, 2011): W29–37. https://doi.org/10.1093/nar/gkr367.

Gao, Xue, Jin-Chun Chen, Qiong Wu, and Guo-Qiang Chen. "Polyhydroxyalkanoates as a Source of Chemicals, Polymers, and Biofuels." *Current Opinion in Biotechnology*, 22/6 Chemical biotechnology and Pharmaceutical biotechnology, 22, no. 6 (December 1, 2011): 768–74. https://doi.org/10.1016/j.copbio.2011.06.005.

Gay, P, D Le Coq, M Steinmetz, E Ferrari, and J A Hoch. "Cloning Structural Gene sacB, Which Codes for Exoenzyme Levansucrase of Bacillus Subtilis: Expression of the Gene in Escherichia Coli." *Journal of Bacteriology* 153, no. 3 (March 1983): 1424–31. https://doi.org/10.1128/jb.153.3.1424-1431.1983.

Geyer, Roland, Jenna R. Jambeck, and Kara Lavender Law. "Production, Use, and Fate of All Plastics Ever Made." *Science Advances* 3, no. 7 (July 19, 2017): e1700782. https://doi.org/10.1126/sciadv.1700782.

Gilchrist, Cameron L M, and Yit-Heng Chooi. "Clinker & Clustermap.Js: Automatic Generation of Gene Cluster Comparison Figures." *Bioinformatics* 37, no. 16 (August 25, 2021): 2473–75. https://doi.org/10.1093/bioinformatics/btab007.

Henderson, Robin A., and Colin W. Jones. "Physiology of Poly-3-Hydroxybutyrate (PHB) Production by Alcaligenes Eutrophus Growing in Continuous Culture." *Microbiology* 143, no. 7 (July 1, 1997): 2361–71. https://doi.org/10.1099/00221287-143-7-2361.

Hosler, D., S. L. Burkett, and M. J. Tarkanian. "Prehistoric Polymers: Rubber Processing in Ancient Mesoamerica." *Science (New York, N.Y.)* 284, no. 5422 (June 18, 1999): 1988–91. https://doi.org/10.1126/science.284.5422.1988.

Juengert, Janina, Stephanie Bresan, and Dieter Jendrossek. "Determination of Polyhydroxybutyrate (PHB) Content in Ralstonia Eutropha Using Gas Chromatography and Nile Red Staining." *BIO-PROTOCOL* 8, no. 5 (2018). https://doi.org/10.21769/BioProtoc.2748.

Kern, Suzanne E., Alexa Price-Whelan, and Dianne K. Newman. "Extraction and Measurement of NAD(P)(+) and NAD(P)H." *Methods in Molecular Biology (Clifton, N.J.)* 1149 (2014): 311–23. https://doi.org/10.1007/978-1-4939-0473-0_26.

Lee, So Jeong, Jiwon Kim, Jung Ho Ahn, Gyeongtaek Gong, Youngsoon Um, Sun-Mi Lee, Kyoung Heon Kim, and Ja Kyong Ko. "Engineering Xylose Utilization in Cupriavidus Necator for Enhanced Poly(3-Hydroxybutyrate) Production from Mixed Sugars." *Bioresource Technology* 418 (February 2025): 131996. https://doi.org/10.1016/j.biortech.2024.131996.

Lemoigne, M. "Produit de Deshydratation et de Polymerisation de l'acide β-Oxybutyrique." *Bull. Soc. Chim. Biol.* 8 (1926): 770–82.

Letunic, Ivica, and Peer Bork. "Interactive Tree Of Life (iTOL) v5: An Online Tool for Phylogenetic Tree Display and Annotation." *Nucleic Acids Research* 49, no. W1 (July 2, 2021): W293–96. https://doi.org/10.1093/nar/gkab301.

Ling, Chen, Guan-Qing Qiao, Bo-Wen Shuai, Karel Olavarria, Jin Yin, Rui-Juan Xiang, Kun-Nan Song, Yun-Hao Shen, Yingying Guo, and Guo-Qiang Chen. "Engineering NADH/NAD+ Ratio in *Halomonas Bluephagenesis* for Enhanced Production of Polyhydroxyalkanoates (PHA)." *Metabolic Engineering* 49 (September 1, 2018): 275–86. https://doi.org/10.1016/j.ymben.2018.09.007.

Macrae, R. M., and J. F. Wilkinson. "Poly- -Hyroxybutyrate Metabolism in Washed Suspensions of Bacillus Cereus and Bacillus Megaterium." *Journal of General Microbiology* 19, no. 1 (August 1, 1958): 210–22. https://doi.org/10.1099/00221287-19-1-210.

Markowitz, Victor M., Frank Korzeniewski, Krishna Palaniappan, Ernest Szeto, Greg Werner, Anu Padki, Xueling Zhao, et al. "The Integrated Microbial Genomes (IMG) System." *Nucleic Acids Research* 34, no. suppl_1 (January 1, 2006): D344–48. https://doi.org/10.1093/nar/gkj024.

McAdam, Blaithín, Margaret Brennan Fournet, Paul McDonald, and Marija Mojicevic. "Production of Polyhydroxybutyrate (PHB) and Factors Impacting Its Chemical and Mechanical Characteristics." *Polymers* 12, no. 12 (December 4, 2020): 2908. https://doi.org/10.3390/polym12122908.

Melnyk, Ryan A., Iain C. Clark, Annette Liao, and John D. Coates. "Transposon and Deletion Mutagenesis of Genes Involved in Perchlorate Reduction in *Azospira Suillum* PS." Edited by Kenneth Nealson and Douglas G. Capone. *mBio* 5, no. 1 (February 28, 2014): e00769-13. https://doi.org/10.1128/mBio.00769-13.

Mifune, Jun, Satoshi Nakamura, and Toshiaki Fukui. "Engineering of Pha Operon on Cupriavidus Necator Chromosome for Efficient Biosynthesis of Poly(3-Hydroxybutyrate-Co-3-Hydroxyhexanoate) from Vegetable Oil." *Polymer Degradation and Stability* 95, no. 8 (August 2010): 1305–12. https://doi.org/10.1016/j.polymdegradstab.2010.02.026.

Minh, Bui Quang, Heiko A. Schmidt, Olga Chernomor, Dominik Schrempf, Michael D. Woodhams, Arndt von Haeseler, and Robert Lanfear. "IQ-TREE 2: New Models and Efficient Methods for Phylogenetic Inference in the Genomic Era." *Molecular Biology and Evolution* 37, no. 5 (May 1, 2020): 1530–34. https://doi.org/10.1093/molbev/msaa015.

Obruca, Stanislav, Petr Sedlacek, and Martin Koller. "The Underexplored Role of Diverse Stress Factors in Microbial Biopolymer Synthesis." *Bioresource Technology* 326 (April 1, 2021): 124767. https://doi.org/10.1016/j.biortech.2021.124767.

Oxley, Jimmie C., James L. Smith, Carolyn Higgins, Patrick Bowden, Jesse Moran, Joe Brady, Carol E. Aziz, and Evan Cox. "Efficiency of Perchlorate Consumption in Road Flares, Propellants and Explosives." *Journal of Environmental Management* 90, no. 11 (August 1, 2009): 3629–34. https://doi.org/10.1016/j.jenvman.2009.06.014.

Poli, Annarita, Paola Di Donato, Gennaro Roberto Abbamondi, and Barbara Nicolaus. "Synthesis, Production, and Biotechnological Applications of Exopolysaccharides and Polyhydroxyalkanoates by Archaea." *Archaea* 2011 (2011): 1–13. https://doi.org/10.1155/2011/693253.

Pötter, Markus, Helena Müller, and Alexander Steinbüchel. "Influence of Homologous Phasins (PhaP) on PHA Accumulation and Regulation of Their Expression by the Transcriptional Repressor PhaR in Ralstonia Eutropha H16." *Microbiology* 151, no. 3 (March 1, 2005): 825–33. https://doi.org/10.1099/mic.0.27613-0.

Redfield, A. C. (1934). On The Proportions of Organic Derivatives in Sea Water and their Relation to the Composition of Plankton. *James Johnson Memorial Volume*, 177–19.

Reyes-Umana, Victor, Sophia D. Ewens, David A. O. Meier, and John D. Coates. "Integration of Molecular and Computational Approaches Paints a Holistic Portrait of Obscure Metabolisms." Edited by Vinayaka R. Prasad. *mBio* 14, no. 6 (December 19, 2023): e00431-23. https://doi.org/10.1128/mbio.00431-23.

Rosenboom, Jan-Georg, Robert Langer, and Giovanni Traverso. "Bioplastics for a Circular Economy." *Nature Reviews Materials* 7, no. 2 (January 20, 2022): 117–37. https://doi.org/10.1038/s41578-021-00407-8.

Sayers, Eric W., Jeff Beck, Evan E. Bolton, J. Rodney Brister, Jessica Chan, Donald C. Comeau, Ryan Connor, et al. "Database Resources of the National Center for Biotechnology Information." *Nucleic Acids Research* 52, no. D1 (January 5, 2024): D33–43. https://doi.org/10.1093/nar/gkad1044.

Scott, Felipe, Luz Yañez, Raúl Conejeros, Blanca Araya, and Alberto Vergara-Fernández. "Two Internal Bottlenecks Cause the Overflow Metabolism Leading to Poly(3-Hydroxybutyrate) Production in Azohydromonas Lata DSM1123." *Journal of Environmental Chemical Engineering* 9, no. 4 (August 2021): 105665. https://doi.org/10.1016/j.jece.2021.105665.

Steinbüchel, A., and H. G. Schlegel. "Physiology and Molecular Genetics of Poly(β-Hydroxyalkanoic Acid) Synthesis in Alcaligenes Eutrophus." *Molecular Microbiology* 5, no. 3 (1991): 535–42. https://doi.org/10.1111/j.1365-2958.1991.tb00725.x.

Steinbüchel, Alexander, and Henry E. Valentin. "Diversity of Bacterial Polyhydroxyalkanoic Acids." *FEMS Microbiology Letters* 128, no. 3 (May 1995): 219–28. https://doi.org/10.1111/j.1574-6968.1995.tb07528.x.

Steinbüchel, Alexander. "3 Polyhydroxyalkanoic Acids" Biomaterials (1991).

Tang, Ruohao, Caihong Weng, Xiaowei Peng, and Yejun Han. "Metabolic Engineering of Cupriavidus Necator H16 for Improved Chemoautotrophic Growth and PHB Production under Oxygen-Limiting Conditions." *Metabolic Engineering* 61 (September 2020): 11–23. https://doi.org/10.1016/j.ymben.2020.04.009.

Thu, Nguyen Thi Tam, Le Huy Hoang, Pham Kien Cuong, Nguyen Viet-Linh, Tran Thi Huyen Nga, Dang Dinh Kim, Yoong Kit Leong, and Le Thi Nhi-Cong. "Evaluation of Polyhydroxyalkanoate (PHA) Synthesis by Pichia Sp. TSLS24 Yeast Isolated in Vietnam." *Scientific Reports* 13, no. 1 (February 23, 2023): 3137. https://doi.org/10.1038/s41598-023-28220-z.

Wang, Liang, Qinghua Liu, Xiang Wu, Yue Huang, Michael J. Wise, Zhanzhong Liu, Wei Wang, Junfeng Hu, and Chunying Wang. "Bioinformatics Analysis of Metabolism Pathways of Archaeal Energy Reserves." *Scientific Reports* 9, no. 1 (January 31, 2019): 1034. https://doi.org/10.1038/s41598-018-37768-0.

Wang, Liang, Jianye Yang, Yue Huang, Qinghua Liu, Yaping Xu, Xue Piao, and Michael J Wise. "Systematic Analysis of Metabolic Pathway Distributions of Bacterial Energy Reserves." *G3 Genes|Genomes|Genetics* 9, no. 8 (August 1, 2019): 2489–96. https://doi.org/10.1534/g3.119.400123.

Wimpenny, Julian W. T., and Anne Firth. "Levels of Nicotinamide Adenine Dinucleotide and Reduced Nicotinamide Adenine Dinucleotide in Facultative Bacteria and the Effect of Oxygen." *Journal of Bacteriology* 111, no. 1 (July 1972): 24–32. https://doi.org/10.1128/jb.111.1.24-32.1972.

Youngblut, Matthew D., Ouwei Wang, Tyler P. Barnum, and John D. Coates. "(Per)Chlorate in Biology on Earth and Beyond." *Annual Review of Microbiology* 70, no. 1 (September 8, 2016): 435–57. https://doi.org/10.1146/annurev-micro-102215-095406.

Zhang, Le, Zicheng Jiang, To-Hung Tsui, Kai-Chee Loh, Yanjun Dai, and Yen Wah Tong. "A Review on Enhancing Cupriavidus Necator Fermentation for Poly(3-Hydroxybutyrate) (PHB) Production From Low-Cost Carbon Sources." *Frontiers in Bioengineering and Biotechnology* 10 (July 19, 2022): 946085. https://doi.org/10.3389/fbioe.2022.946085.

Zheng, Jiajia, and Sangwon Suh. "Strategies to Reduce the Global Carbon Footprint of Plastics." *Nature Climate Change* 9, no. 5 (May 2019): 374–78. https://doi.org/10.1038/s41558-019-0459-z.

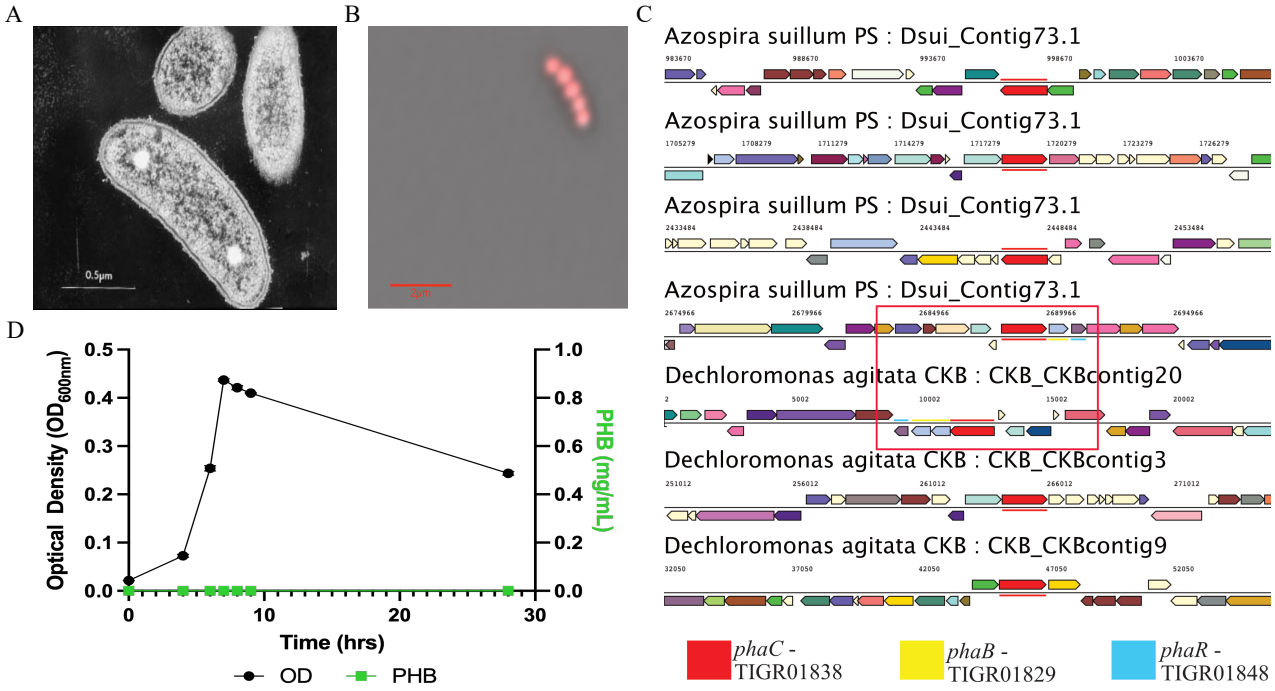


**Figure 1 |** Microscopic and comparative genomic analysis of PHA production in *Dechloromonas agitata* CKB and *Azospira suillum* PS. (**A**) Transmission electron micrograph (TEM) of *D. agitata* CKB adapted from Bruce et al., 1995, showing electron-dense inclusions consistent with PHA granules. (**B**) Confocal fluorescence microscopy image of Nile Red-stained A. suillum PS overlaid with transmitted light, highlighting intracellular PHA granules. (**C**) Gene neighborhood analysis of phaC loci in CKB and PS, with neighboring PHA biosynthesis genes highlighted where present in the red box. (**D**) Growth ($OD_{600}$) and absolute PHB production (mg/mL) by *A. suillum* PS during aerobic cultivation under nitrogen replete growth conditions.

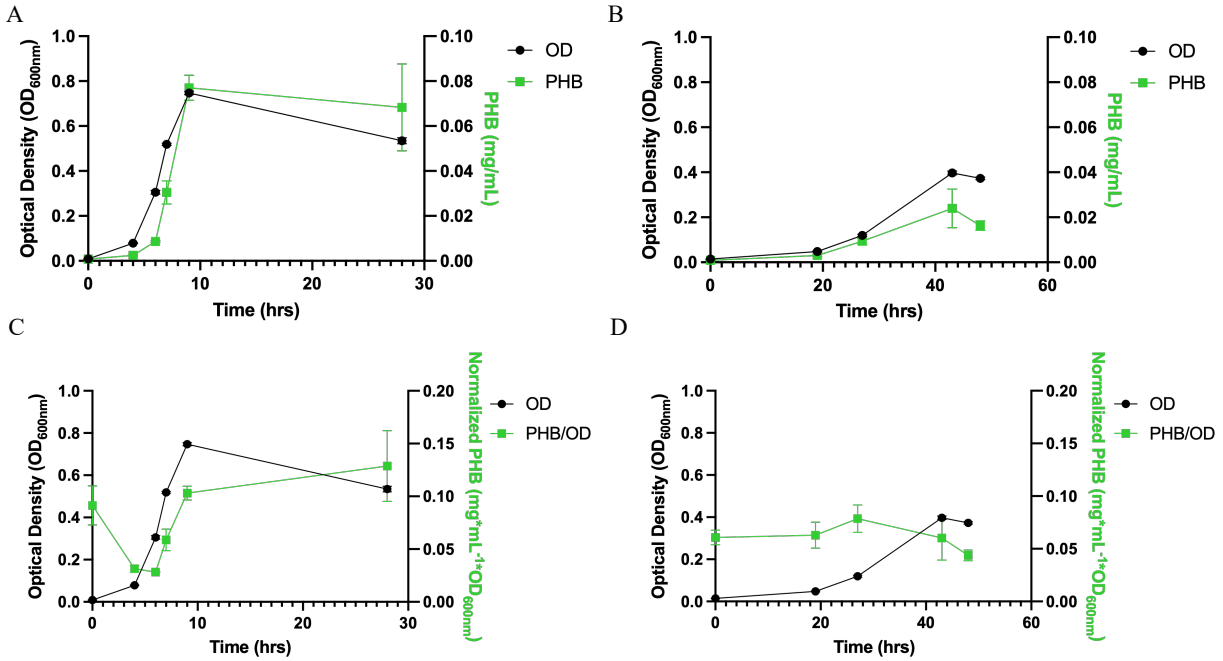


**Figure 2 |** PHA production by *Azospira suillum* PS across electron acceptors with acetate as the electron donor under moderate nitrogen deplete conditions**. (A)** Growth ($OD_{600}$) and absolute PHB production (mg/mL) during aerobic cultivation. **(B)** Growth ($OD_{600}$) and absolute PHB production (mg/mL) during perchlorate-respiring growth. **(C)** Growth ($OD_{600}$) and normalized PHB production (mg $mL^{-1}$ $OD_{600}^{-1}$) under aerobic conditions. **(D)** Growth ($OD_{600}$) and normalized PHB production (mg $mL^{-1}$ $OD_{600}^{-1}$) during perchlorate respiration.

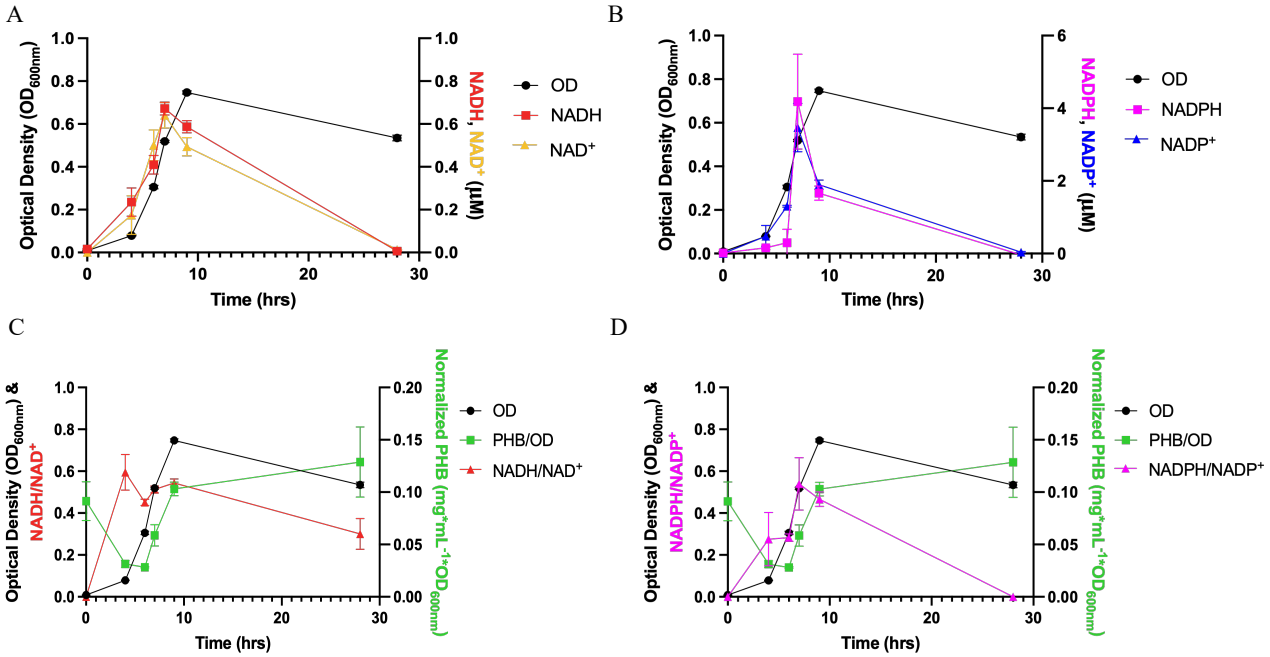


**Figure 3 |** Normalized PHA production and intracellular redox state of *Azospira* suillum PS grown aerobically on acetate. **(A)** Growth ($OD_{600}$) and absolute intracellular concentrations of NADH and $NAD^+$ (µM). **(B)** Growth and absolute concentrations of NADPH and $NADP^+$ (µM). **(C)** Growth, normalized PHB production (mg $mL^{-1}$ $OD_{600}^{-1}$), and the NADH/$NAD^+$ ratio. **(D)** Growth, normalized PHB production, and the NADPH/$NADP^+$ ratio.

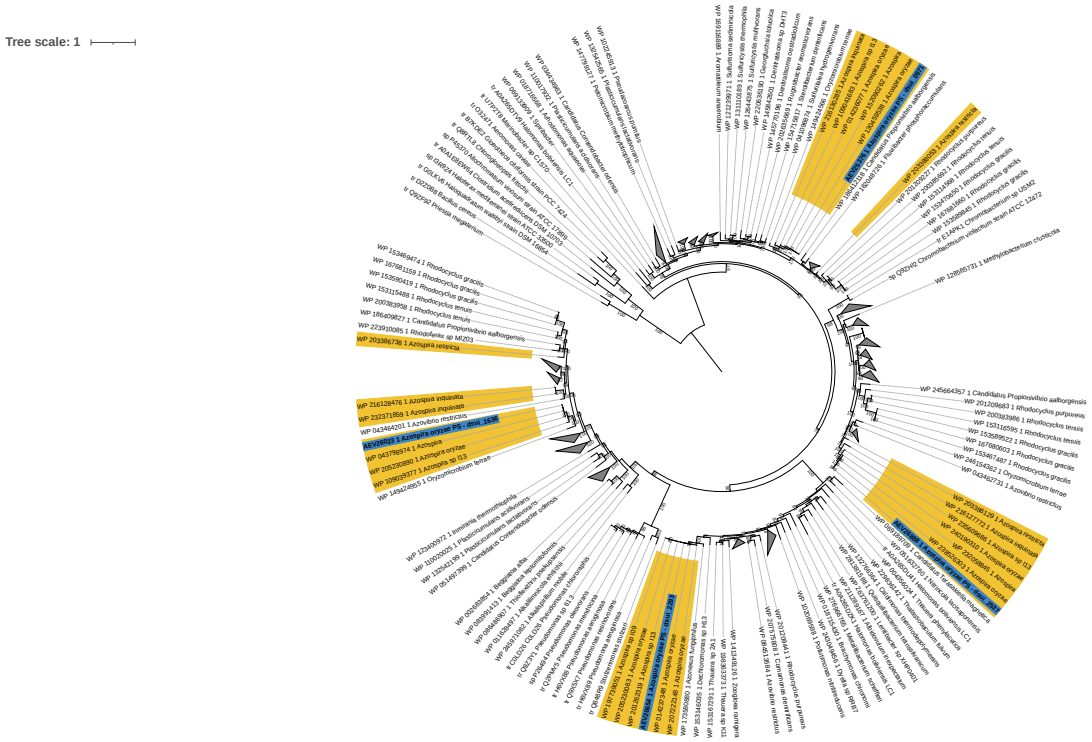


**Figure 4 |** PhaC protein phylogeny within the genus *Azospira***.** Maximum likelihood phylogenetic tree of PhaC protein sequences from members of the genus *Azospira*. Bootstrap support values (n = 1000 replicates) are shown at each node. Branches corresponding to *Azospira* species are highlighted in yellow, and those from A. suillum PS are further annotated in blue. Tip labels include the GenBank protein accession number followed by the corresponding NCBI organism name.

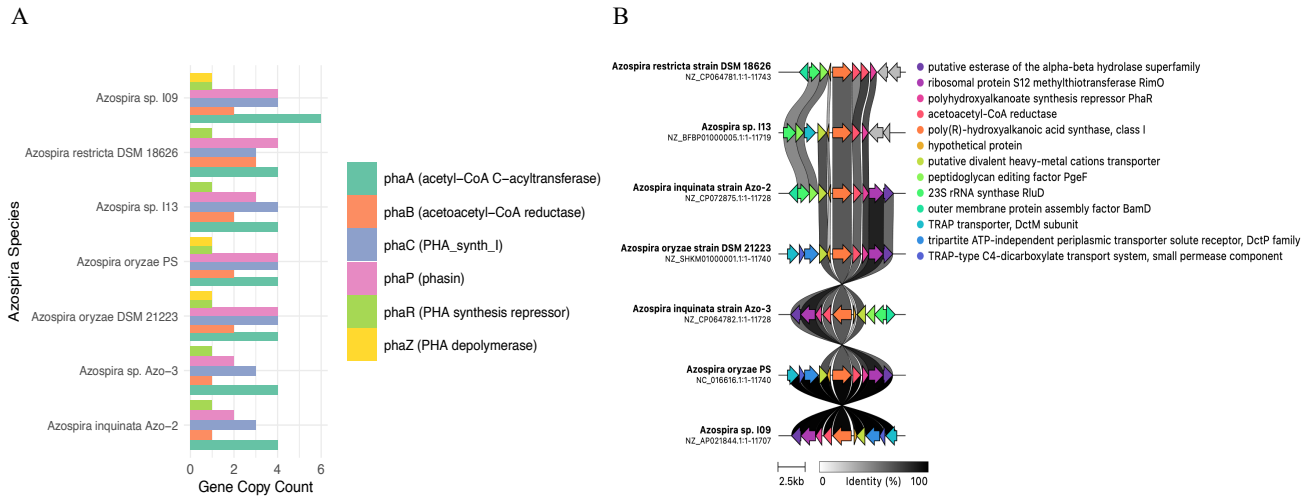


**Figure 5** | Distribution of PHA-associated genes across the genus *Azospira*. **(A)** Presence and distribution of all identified PHA-associated genes across sequenced genomes within the genus *Azospira*. **(B)** Nucleotide identity percentages for the phaC biosynthetic cluster co-localized with phaB and phaR across *Azospira* species, highlighting variation in conservation of this operon.

610 **Table 1 |** Polyhydroxyalkanoate methyl esters produced by ***Azospira suillum*** PS when grown on
611 complex or defined media. Summary of PHA monomers identified in *A. suillum* PS when cultivated
612 on complex media (acetate, lactate, pyruvate with yeast extract) or defined acetate minimal medium.
613 PS locus tags corresponding to each *phaC* gene are listed in Supplementary Table 5.

| **Strains** | **PHB** | **PHV** | **PHHX** |
|---|---|---|---|
| WT | + | - | - |
| *ΔphaC1* | + | - | - |
| *ΔphaC2* | + | - | - |
| *ΔphaC3* | + | - | - |
| *Δ(phaC1-phaC2)* | + | - | - |
| *Δ(phaC1-phaC3)* | + | - | - |
| *Δ(phaC2-phaC3)* | + | - | - |
| *Δ(phaC1-phaC2-phaC3)* | + | - | - |

614